8-1-2007

Bifurcation scenarios in semiconductor lasers subject to optical injection

Rachel Marilley

Bifurcation scenarios in semiconductor lasers subject to optical injection

By

Rachel Marilley

Submitted in partial fulfillment of the requirements for the degree
Master of Science
at
Rochester Institute of Technology
Rochester, NY
August 2007

Abstract

In the thesis we examine the dynamics of semiconductor lasers subject to optical injection. We study typical bifurcation scenarios, namely the saddle-node and Hopf bifurcations associated with this system. First, the system is investigated analytically, then numerical simulations verify our analytical conclusions.

Chapter 1

Analytic Results

1.1 Introduction

In this project we will be examining some aspects of the dynamics of semiconductor lasers subject to optical injection, especially some bifurcation scenarios. First, we review the basics of operation of semiconductor lasers. A laser diode is a laser where the active medium is a semiconductor similar to that in a light-emitting diode. The most common type of laser diode is formed from a $p-n$ junction and powered by an electrical current. There is a layer of electron-rich material (n-type) over a layer of holes-rich (p-type) material. Interaction between electrons and holes occurs in a central layer to generate photons, and these generated photons further interact with more electrons and holes, causing stimulated emission, and strengthening the photon beam. The current applied across the laser is the pump current which offers the initial energy for the electron-hole interaction (see Figure 1).

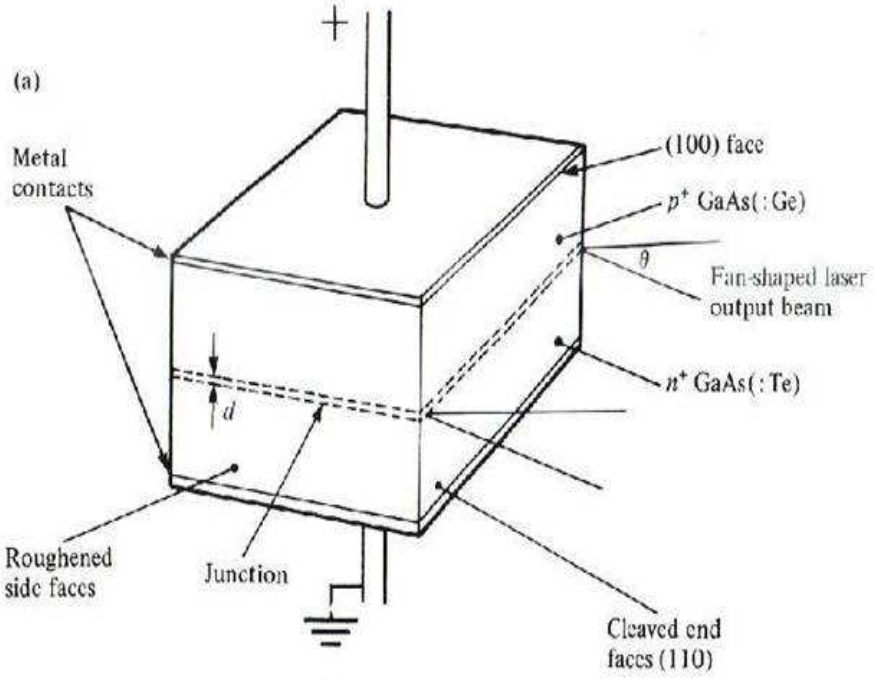

Figure 1: Semiconductor laser structure

Semiconductor lasers are used in various fields, particularly in optical data recording and optical fiber communications. In the literature, various scalings of a model for a laser with optical injection are used ([1, 5, 8]). We will formulate our equations in the next section.

1.2 The System

The differential equation system describing the operation of semiconductor lasers with optical injection is given in the following complex form ([2]):

$$\dot{\mathcal{E}} = (1 + i\alpha)N\mathcal{E} + \eta e^{i\Omega t} \tag{1.1}$$

$$T\dot{N} = P - N - (1 + 2N)|\mathcal{E}|^2, \tag{1.2}$$

Here $\mathcal{E}$ is the complex electric field and N is the carrier density above threshold. The parameters are the following: η is the injection strength, α is the

linewidth enhancement factor, Ω is the detuning, T is the ratio of photon and carrier lifetime and P is the pumping current.

We will put this into real form by breaking the complex electric field into its absolute value and phase:

$$\mathcal{E}(t) = E(t)e^{i\phi(t)}.$$

Differentiating this expression and substituting $\psi(t) = \Omega t - \phi(t)$ we obtain the following single-mode rate equation model:

$$\begin{aligned} \dot{E} &= NE + \eta\cos\psi && (1.3)\\ \dot{\psi} &= \Omega - \alpha N - \frac{\eta}{E}\sin\psi && (1.4)\\ T\dot{N} &= P - N - (1+2N)E^2, && (1.5) \end{aligned}$$

where now E is the amplitude of the electrical field and ψ is the phase difference between master and slave electrical fields.

Equation (1.3) describes the evolution of the amplitude of the electric field, (1.4) models the phase difference between electrical fields and (1.5) models the carrier density.

1.3 Steady States

It is important to determine the steady state solutions for the single-mode rate equation (1.3-1.5) in order to investigate its stability properties. These solutions correspond to solutions of the original system (1.1-1.2) in the form $(\mathcal{E}, N) = (E_s e^{i(\Omega t - \psi_s)}, N_s)$. As we see this means that the absolute value of the complex electric field is constant, which means the laser operates with constant intensity.

First we find the equilibrium points.

$$\begin{aligned} N_s E_s + \eta\cos\psi_s &= 0 && (1.6)\\ \Omega - \alpha N_s - \frac{\eta}{E_s}\sin\psi_s &= 0 && (1.7)\\ P - N_s - (1+2N_s)E_s^2 &= 0 && (1.8) \end{aligned}$$

We will solve the system for the constants N_s, E_s, and ψ_s.

Multiply (1.6) with α and (1.7) with E_s and add the two equations:

$$\eta\sin\psi_s - \alpha\eta\cos\psi_s = \Omega E_s.$$

This transforms to

$$\eta\sqrt{1+\alpha^2}(\frac{1}{\sqrt{1+\alpha^2}}\sin\psi_s - \frac{\alpha}{\sqrt{1+\alpha^2}}\cos\psi_s) = \Omega E_s,$$

so

$$\eta\sqrt{1+\alpha^2}\sin(\psi_s - \arctan\alpha) = \Omega E_s. \tag{1.9}$$

Also, by multiplying (1.7) with E_s and adding the squares of the appropriate expressions,

$$\eta^2 = (N_s E_s)^2 + (\Omega E_s - \alpha N_s E_s)^2 = E_s^2[N_s^2 + (\Omega - \alpha N_s)^2]. \tag{1.10}$$

From (1.8), we can see that at the equilibrium

$$E_s^2 = \frac{P - N_s}{1 + 2N_s}. \tag{1.11}$$

Now from (1.11) we can substitute E_s^2 into (1.10) and create a cubic equation for N_s, then we can find E_s from (1.11) and then (1.9) gives us ψ_s.

The cubic we obtain this way is given by

$$N_s^3(1+\alpha^2) + N_s^2(-P - \alpha^2 P - 2\alpha\Omega) + N_s(2\eta^2 + 2\alpha\Omega P + \Omega^2) + \eta^2 - P\Omega^2 = 0. \tag{1.12}$$

The structure of finding a steady-state solution is clear now: we can obtain N_s from (1.12), then (1.11) gives us E_s and then (1.9) provides us with ψ_s.

This cubic equation will have either 1 or 3 real roots (counting with multiplicity). The parameter we will use as bifurcation parameter will usually be the injection strength η. First we will investigate the change from 1 real solution to 3 real solutions. This will give us a saddle-node bifurcation: a new equilibrium solution pops up from "nowhere" and bifurcates into two equilibrium solutions. This corresponds to different intensity operating behavior for the laser. We will explore this briefly in the next section.

1.4 Saddle-node Bifurcation for the Cubic

Generally, for a cubic equation with positive leading coefficient the scenario is depicted on the following figure:

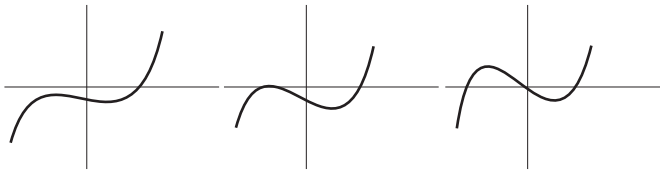

Figure 2: Saddle-node bifurcation for the cubic: 1 real root, 3 real roots (one with multiplicity 2), 3 real roots.

We can see that the change from 1 real solution to 3 real solutions will happen when the smaller zero for the derivative of the function is a zero of the original function as well. If the cubic is given by

$$ax^3 + bx^2 + cx + d, \qquad a > 0,$$

then the derivative is

$$3ax^2 + 2bx + c$$

and the zero in question is

$$x = \frac{-2b - \sqrt{4b^2 - 12ac}}{6a} = \frac{-b - \sqrt{b^2 - 3ac}}{3a}.$$

This means that the bifurcation will occur when

$$a(\frac{-b - \sqrt{b^2 - 3ac}}{3a})^3 + b(\frac{-b - \sqrt{b^2 - 3ac}}{3a})^2 + c\frac{-b - \sqrt{b^2 - 3ac}}{3a} + d = 0.$$

In our case, we have the following values: $a = 1 + \alpha^2 > 0$, $b = -P - \alpha^2 P - 2\alpha\Omega$, $c = 2\eta^2 + 2\alpha\Omega P + \Omega^2$ and $d = \eta^2 - P\Omega^2$.

In our computations we will use the physically meaningful values $\alpha = 5$ and $P = 1$ first. On the next figure we plot the Ω and η pairs where this saddle-node bifurcation occurs for the given values of α and P.

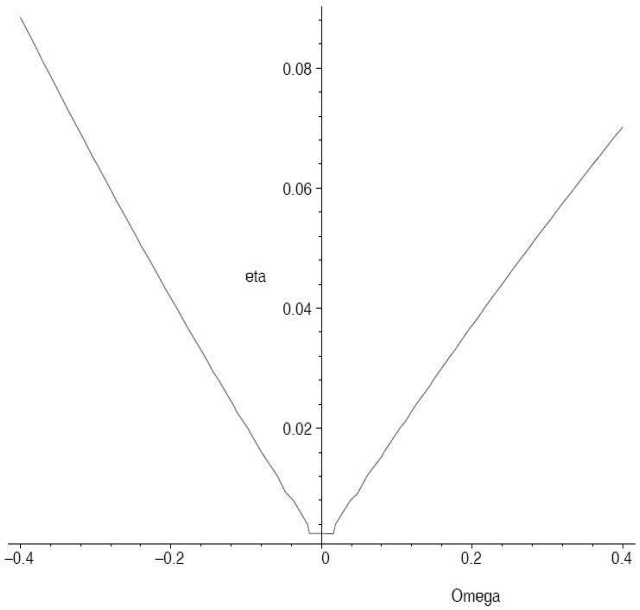

Figure 3: Saddle-node bifurcation for the laser equation, $\alpha = 5$, $P = 1$

For a given Ω value the curve gives the corresponding η value where new equilibria appears.

Generally, in a saddle-node bifurcation one of the equilibria appearing is stable, the other is unstable. We will see numerical confirmation of this later, when we evaluate the new equilibria and the corresponding eigenvalues. We will also simulate the solutions to the differential equation system. We will also see that the stable equilibrium from the new equilibrium pair undergoes a Hopf bifurcation for a slightly higher η value. To establish this claim we will now study the eigenvalues of the linearized system at the above mentioned equilibrium positions.

1.5 Eigenvalues

Let us linearize (1.3), (1.4), (1.5) at the steady state (1.6), (1.7), (1.8). We evaluate the Jacobian of the single-mode rate equation system (1.3-1.5):

$$\mathcal{J} = \begin{bmatrix} N & -\eta \sin\psi & E \\ \frac{\eta}{E^2}\sin\psi & -\frac{\eta}{E}\cos\psi & -\alpha \\ -\frac{2(1+2N)E}{T} & 0 & -\frac{1+2E^2}{T} \end{bmatrix}. \tag{1.13}$$

At the equilibrium (E_s, ψ_s, N_s)

$$\mathcal{J} = \begin{bmatrix} N_s & -\eta \sin\psi_s & E_s \\ \frac{\eta}{E_s^2}\sin\psi_s & -\frac{\eta}{E_s}\cos\psi_s & -\alpha \\ -\frac{2(1+2N_s)E_s}{T} & 0 & -\frac{1+2E_s^2}{T} \end{bmatrix}. \tag{1.14}$$

Now we will try to find the characteristic equation at the above equilibrium points. First, we eliminate ψ_s using (1.6) and (1.7). We obtain the Jacobian

$$\mathcal{J} = \begin{bmatrix} N_s & E_s(\alpha N_s - \Omega) & E_s \\ \frac{\Omega-\alpha N_s}{E_s} & N_s & -\alpha \\ -\frac{2(1+2N_s)E_s}{T} & 0 & -\frac{1+2E_s^2}{T} \end{bmatrix} \tag{1.15}$$

We use the notation $\varepsilon \equiv 1/T$. The characteristic polynomial is then given by

$$p(\lambda) = |\,\mathcal{J} - \lambda I| = \begin{vmatrix} N_s - \lambda & E_s(\alpha N_s - \Omega) & E_s \\ \frac{\Omega-\alpha N_s}{E_s} & N_s - \lambda & -\alpha \\ -2\varepsilon(1+2N_s)E_s & 0 & -\varepsilon(1+2E_s^2) - \lambda \end{vmatrix} \tag{1.16}$$

We obtain a cubic polynomial:

$$-p(\lambda) = \lambda^3 + A_1\lambda^2 + A_2\lambda + A_3,$$

where the coefficients are the following:

$$\begin{aligned} A_1 &= \varepsilon(1+2E_s^2) - 2N_s \\ A_2 &= -2\varepsilon N_s(1+2E_s^2) + N_s^2 + 2\varepsilon E_s^2(1+2N_s) + (\Omega - \alpha N_s)^2 \\ A_3 &= \varepsilon N_s^2(1+2E_s^2) + 2\alpha\varepsilon E_s^2(\Omega - \alpha N_s)(1+2N_s) - 2\varepsilon N_s E_s^2(1+2N_s) \\ &\quad +\varepsilon(1+2E_s^2)(\Omega - \alpha N_s)^2 \end{aligned}$$

Using (1.11), we obtain the coefficients depending only on N_s:

$$\begin{aligned} A_1 &= \varepsilon\frac{1+2P}{1+2N_s} - 2N_s \\ A_2 &= N_s^2 + (\Omega - \alpha N_s)^2 + 2\varepsilon(P - N_s) - 2\varepsilon N_s\frac{1+2P}{1+2N_s} \\ A_3 &= \varepsilon N_s^2\frac{1+2P}{1+2N_s} + 2\varepsilon\alpha(P - N_s)(\Omega - \alpha N_s) - 2\varepsilon N_s(P - N_s) \\ &\quad +\varepsilon\frac{1+2P}{1+2N_s}(\Omega - \alpha N_s)^2 \end{aligned}$$

The eigenvalues at a given equilibrium point are given now by the equation

$$-p(\lambda) = \lambda^3 + A_1\lambda^2 + A_2\lambda + A_3 = 0. \tag{1.17}$$

In the next section we investigate the stability of our equilibria.

1.6 Stability Boundaries

According to the Routh-Hurwitz stability criterion, each solution of (1.17) has negative real part if the following matrix has positive leading minors ([6]):

$$\begin{bmatrix} A_1 & 1 & 0 \\ A_3 & A_2 & A_1 \\ 0 & 0 & A_3 \end{bmatrix}$$

This means that $A_1 > 0$, $A_1A_2 - A_3 > 0$ and $A_3 > 0$ implies that all eigenvalues have negative real part and the equilibrium is (asymptotically) stable.

We lose stability when an eigenvalue crosses the imaginary axis as we change the bifurcation parameter η.

This can happen in two ways: either the eigenvalue crossing over the imaginary axis is real, which means that $A_3 = 0$ at this point, or a complex pair of eigenvalues is crossing over the imaginary axis simultaneously, which happens when $A_1A_2 = A_3$. (We will elaborate on these equations later.) In both cases, we first solve the coefficient equation ($A_3 = 0$ or $A_1A_2 = A_3$) for $\Omega - \alpha N_s$ (both of these equations are quadratic for this expression),

then plugging this back into (1.10) we get a parametric representation of the boundary of the stability region in the $\eta - \Omega$ plane, parametrized by N_s.

Let us check the first inequality $A_1 > 0$ briefly. This happens when

$$A_1 = \varepsilon \frac{1+2P}{1+2N_s} - 2N_s > 0.$$

This is the same as

$$4N_s^2 + 2N_s - \varepsilon(1+2P) < 0,$$

which happens when

$$-\frac{1}{4} - \sqrt{\frac{1}{16} + \varepsilon\frac{1+2P}{4}} < N_s < -\frac{1}{4} + \sqrt{\frac{1}{16} + \varepsilon\frac{1+2P}{4}}.$$

We will only use N_s parameter values satisfying this inequality.

1.6.1 Real Eigenvalue Crossing

First, we analyze the real eigenvalue crossing. Again, this happens when one real eigenvalue crosses through the origin. At this point clearly $\lambda = 0$ solves (1.17), so $p(0) = A_3 = 0$.

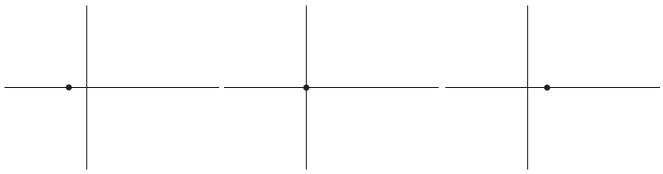

Figure 4: Real Crossing

In this case

$$\begin{aligned} A_3 &= \varepsilon N_s^2 \frac{1+2P}{1+2N_s} + 2\varepsilon\alpha(P-N_s)(\Omega - \alpha N_s) - 2\varepsilon N_s(P-N_s) + \\ &\quad + \varepsilon\frac{1+2P}{1+2N_s}(\Omega - \alpha N_s)^2 = 0, \end{aligned}$$

which simplifies to

$$\begin{aligned} &(1+2P)(\Omega - \alpha N_s)^2 + 2\alpha(P-N_s)(1+2N_s)(\Omega - \alpha N_s) + \\ &+ N_s^2(1+2P) - 2N_s(P-N_s)(1+2N_s) = 0. \end{aligned}$$

Solving this second order equation for $\Omega - \alpha N_s$, we get

$$\Omega - \alpha N_s =$$

$$= \frac{-\alpha(P-N_s)(1+2N_s)}{1+2P}$$

$$\pm \frac{\sqrt{\alpha^2(P-N_s)^2(1+2N_s)^2 - (1+2P)(N_s^2(1+2P) - 2N_s(P-N_s)(1+2N_s))}}{1+2P}.$$

So

$$\Omega = \frac{2\alpha N_s(1+N_s) - \alpha P}{1+2P}$$

$$\pm \frac{\sqrt{\alpha^2(P-N_s)^2(1+2N_s)^2 - (1+2P)(N_s^2(1+2P) - 2N_s(P-N_s)(1+2N_s))}}{1+2P}.$$

Also,

$$\eta = \sqrt{\frac{P-N_s}{1+2N_s}}\sqrt{N_s^2 + (\Omega - \alpha N_s)^2}.$$

This way, we got a one-parameter curve in the $\Omega - \eta$ plane which describes the stability boundary. The parameter is N_s. We will see immediately when we compare the above given curve with the saddle-node bifurcation curve that the saddle-node bifurcation curve masks this curve in the sense that that curve is above our "real crossing" curve, so in the numerical simulations we will not see this case: the saddle-node bifurcation does not take place before we reach the level of the "real crossing" bifurcation. The bifurcation we will be really interested in is the other one: when the stable equilibrium popping up in the saddle-node bifurcation undergoes a secondary (Hopf) bifurcation.

1.6.2 Complex Pair of Eigenvalues Crossing

Now we do a similar analysis for the Hopf bifurcation, where a complex pair of eigenvalues crosses the imaginary axis. This happens when we have one real eigenvalue λ_1 and a complex conjugate pair, $a \pm i\omega$. We cross the imaginary axis when $a = 0$: in this case

$$-p(\lambda) = (\lambda - \lambda_1)(\lambda - i\omega)(\lambda + i\omega) = (\lambda - \lambda_1)(\lambda^2 + \omega^2) = \lambda^3 - \lambda_1\lambda^2 + \omega^2\lambda - \lambda_1\omega^2.$$

Comparing this with the original characteristic polynomial we obtain that

$$-\lambda_1 = A_1 \qquad \omega^2 = A_2 \qquad -\lambda_1\omega^2 = A_3.$$

This shows that we will have the eigenvalue crossing when $A_1A_2 = A_3$. (Also, the real eigenvalue $\lambda_1 < 0$ according to the first leading minor inequality $A_1 > 0$. We remark that the frequency of the appearing periodic solutions is $\omega = \sqrt{A_2}$.

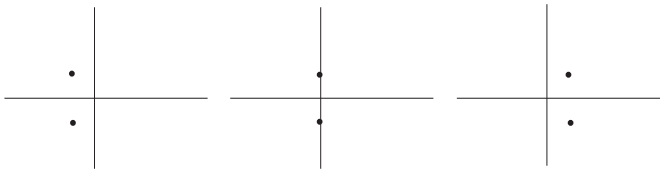

Figure 5: Complex Crossing

For our system this happens when

$$(\varepsilon\frac{1+2P}{1+2N_s} - 2N_s)(N_s^2 + (\Omega - \alpha N_s)^2 + 2\varepsilon(P - N_s) - 2\varepsilon N_s\frac{1+2P}{1+2N_s}) =$$

$$= \varepsilon N_s^2\frac{1+2P}{1+2N_s} + 2\varepsilon\alpha(P-N_s)(\Omega-\alpha N_s) - 2\varepsilon N_s(P-N_s) + \varepsilon\frac{1+2P}{1+2N_s}(\Omega-\alpha N_s)^2.$$

This means that

$$2N(\Omega - \alpha N)^2 + 2\varepsilon\alpha(P - N)(\Omega - \alpha N) +$$

$$+[2N\varepsilon(P-N) + 2N^3 + 2N\varepsilon^2\frac{(1+2P)^2}{(1+2N)^2} - 4N^2\varepsilon\frac{1+2P}{1+2N} - 2\varepsilon^2\frac{(P-N)(1+2P)}{1+2N}] = 0$$

We can solve this second order equation for $\Omega - \alpha N_s$ again and obtain that

$$\Omega - \alpha N_s =$$

$$= \frac{-2\varepsilon\alpha(P - N_s)}{4N_s} \pm$$

$$\frac{\sqrt{4\varepsilon^2\alpha^2(P - N_s)^2 - 8N_s(2N_s\varepsilon(P - N_s) + 2N_s^3 + \frac{1+2P}{1+2N_s}(2N_s\varepsilon^2\frac{1+2P}{1+2N_s} - 4N_s^2\varepsilon - 2\varepsilon^2(P - N_s)))}}{4N_s}.$$

Also, again

$$\eta = \sqrt{\frac{P - N_s}{1 + 2N_s}}\sqrt{N_s^2 + (\Omega - \alpha N_s)^2}.$$

On the next figure we can see these curves for $\alpha = 5$, $P = 1$ and $\varepsilon = 0.001$. The N_s parameter values vary between -0.5 and 0.02, so we will have to look

for these N_s values in the cubic when investigating the loss of stability. As we mentioned earlier, we will primarily be interested in the Hopf bifurcation of the equilibria appearing after the saddle-node bifurcation. These will have to show up at physically meaningful values of Ω and η, so on these figures we only use the branch corresponding to the plus sign in the solution.

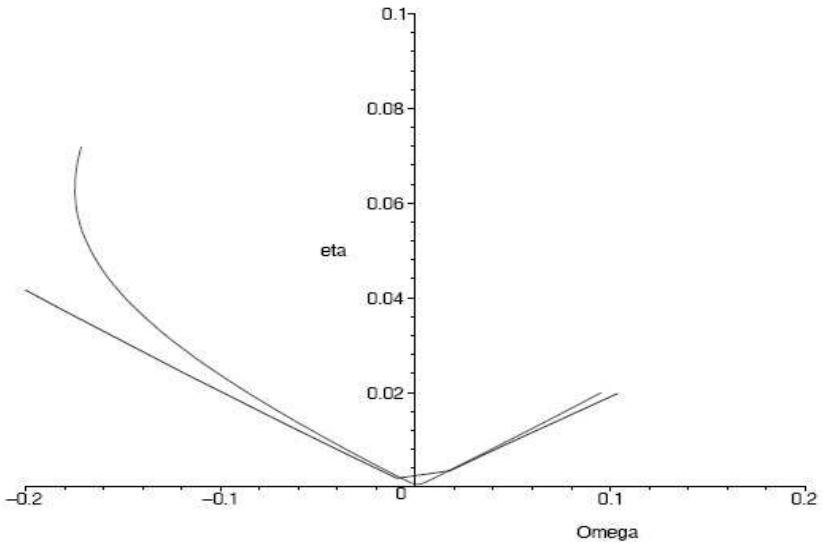

Figure 6: The stability boundaries on the $\Omega - \eta$ plane

We will also see later when we numerically examine these systems that the above scenario will occur only for negative detuning values; the reason is that in the Routh-Hurwitz criterion the assumption $A_1 > 0$ will happen only for these values.

We obtained analytically that the expected scenario is the following: first, a new pair of equilibria appears in a saddle-node bifurcation when we raise the level of η. One of these is stable, the other one is unstable. By raising the level of η further the stable equilibrium loses its stability in a Hopf bifurcation. The next figure shows the behavior. Also, observe that for certain Ω values raising the η level can bring stability back.

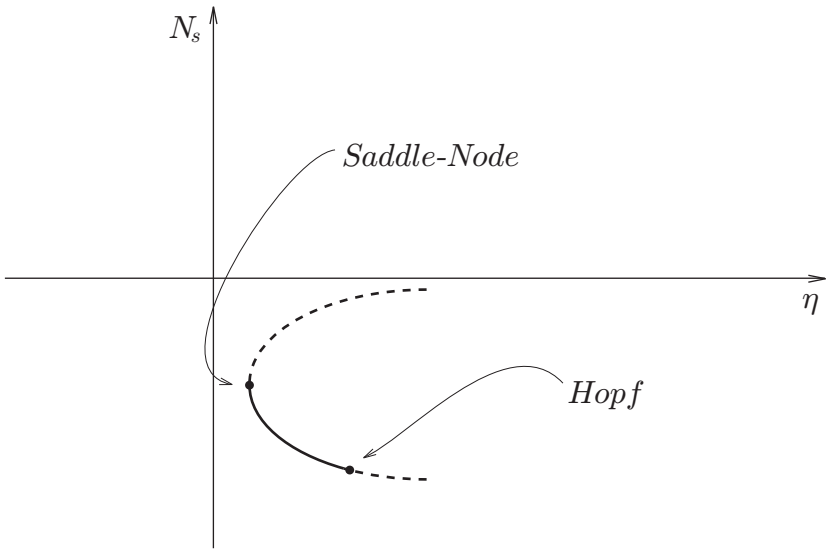

Figure 7: The bifurcations and the stability properties of equilibria

Chapter 2

Numerical Results

2.1 Bifurcations

In this section we will systematically consider parameter values which will support our claims for some of the above-mentioned bifurcations.

The physically meaningful values of the linewidth enhancement factor $\alpha = 5$, pump current $P = 1$ and the ratio of photon and carrier lifetime $T = 1000$ will be used throughout. It is of course an exciting question how these parameters change the behavior of our system; this could be the topic of an incomparably more difficult and lengthy bifurcation analysis. We mention that the description of bifurcation scenarios for ultra small linewidth enhancement factors α is actively being investigated presently, as this question is fundamental in the behavior of quantum dot lasers. We will compare some of the aspects at the end of this section.

Let us first consider the value of the detuning $\Omega = -0.1$. Our bifurcation parameter will be the injection strength η. We start with $\eta = 0.02$. We use MATLAB for our computations; the code for the various computations can be found in the appendix.

The roots of the cubic equation for N_s are (1.12)

$$\begin{aligned} &0.99995556945283 \\ &-0.01920855395718 + 0.00052785410752\mathtt{i} \\ &-0.01920855395718 - 0.00052785410752\mathtt{i}. \end{aligned}$$

We can check on Figure 3 that we are still below the saddle-node bifurcation curve, so we only have one real root for the cubic and one equilibrium

position of the original differential equation system. The eigenvalues of the Jacobian (1.15) at the only real root are

$$\begin{aligned} &0.99995552586089 + 5.09977784742040\mathtt{i} \\ &0.99995552586089 - 5.09977784742040\mathtt{i} \\ -&0.00099994243738. \end{aligned}$$

This shows that this equilibrium solution is unstable, as the real part of the complex conjugate pair is positive. One solution starting close to this equilibrium is shown as a function of time and as a phase-space curve in the E-ψ-N-space on the next Figure. On all of the time integration figures, the horizontal axis is time.

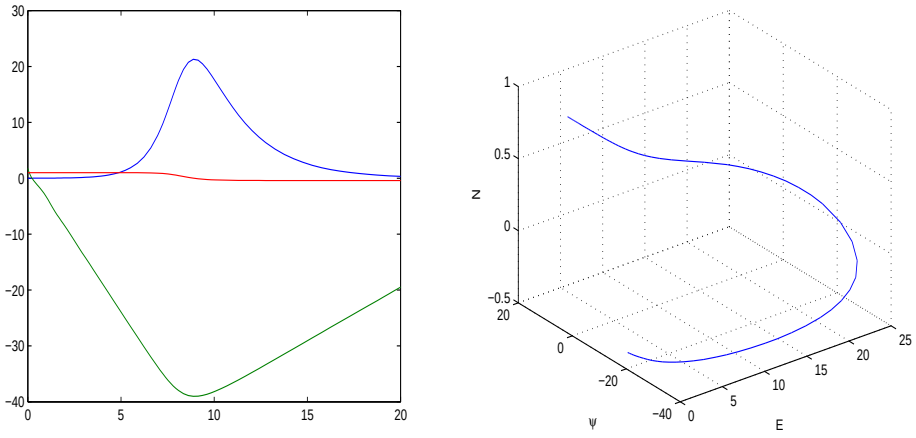

Figure 8: Solution when $\Omega = -0.1$ and $\eta = 0.02$.

Let us raise the injection level above the saddle-node curve now at this detuning value. We choose $\eta = 0.022$. We obtain that the roots of the cubic (1.12) are

$$\begin{aligned} &0.99994623838796 \\ -&0.02086811581976 \\ -&0.01753966102974. \end{aligned}$$

We can see that now we have three real roots for N_s, which translates to three equilibrium solutions. One of the equilibria obtained from the saddle-node bifurcation is stable, the other unstable: the eigenvalues of the Jacobian

(1.15) at the first steady state of the new pair are

$$\begin{aligned} &-0.00365490519164 + 0.048361386073 61\mathrm{i} \\ &-0.00365490519164 - 0.048361386073 61\mathrm{i} \\ &-0.03755708329216, \end{aligned}$$

and at the second steady state of the new pair are

$$\begin{aligned} &-0.03023757953229 + 0.055105349241 01\mathrm{i} \\ &-0.03023757953229 - 0.055105349241 01\mathrm{i} \\ &\ \ 0.02228677315293, \end{aligned}$$

which shows the validity of our claim about their stability properties. We also show time integration results at these equilibria.

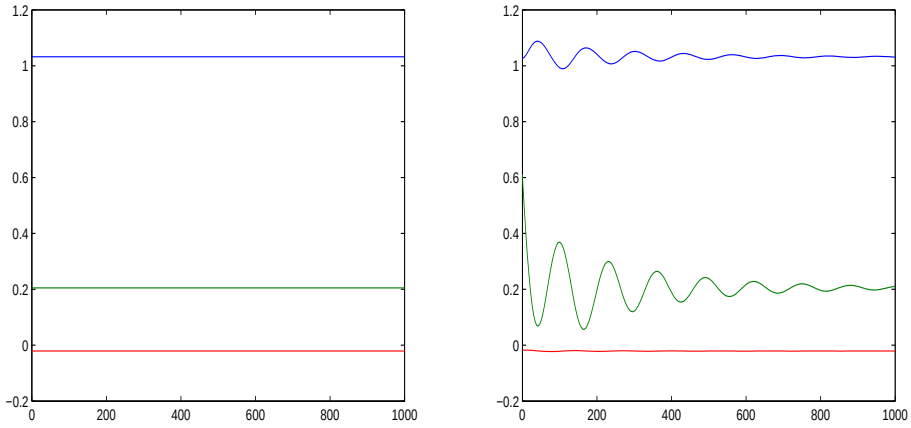

Figure 9: Solutions when $\Omega = -0.1$ and $\eta = 0.022$; saddle-node bifurcation equilibria.

The phase-space picture also shows that one of these new equilibria is unstable, the other stable: a solution starting close to the unstable is attracted to the stable one.

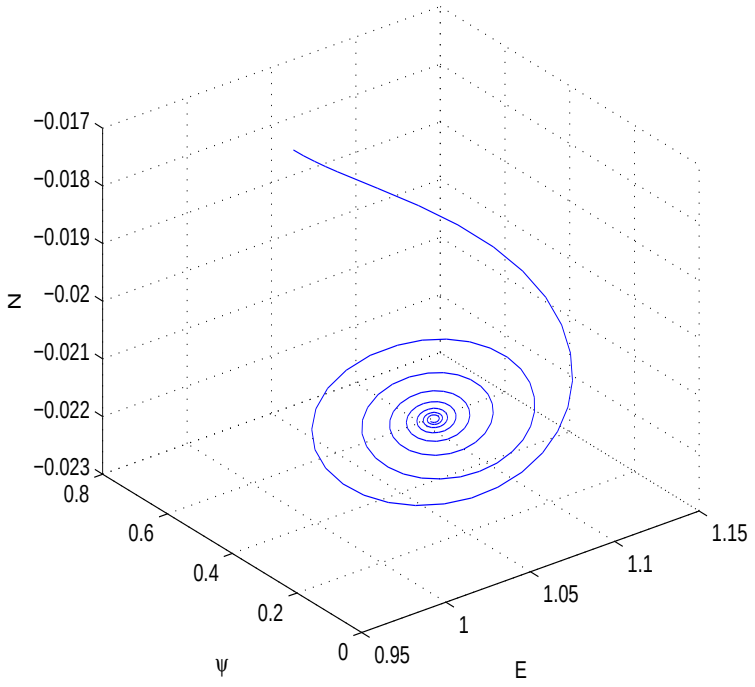

Figure 10: Phase-space plot when $\Omega = -0.1$ and $\eta = 0.022$; the solution leaves the unstable equilibrium and is attracted to the stable one.

Now we raise the level of the injection again, this time above the Hopf bifurcation curve on Figure 6. We expect that the (up to this point) stable equilibrium obtained from the saddle-node bifurcation loses its stability and becomes unstable as the complex pair of eigenvalues corresponding to this steady state will cross over to the positive real part half of the complex plane. We choose $\eta = 0.024$. We obtain that the roots of the cubic (1.12) are

$$\begin{aligned} &0.99993601839135 \\ &-0.02167028854173 \\ &-0.01672726831115. \end{aligned}$$

The eigenvalues at the second of these equilibria are now

$$\begin{aligned} &0.00049720710892 + 0.052588585746 70\mathrm{i} \\ &0.00049720710892 - 0.052588585746 70\mathrm{i} \\ &-0.04747090354775. \end{aligned}$$

We can see that the hitherto stable solution really loses its stability, according to the eigenvalues. Time integration and phase-space plot at this equilibrium changes to the following:

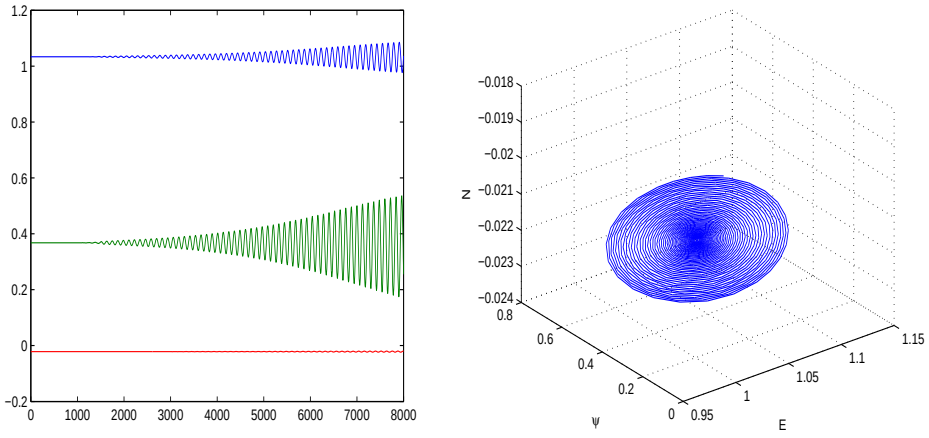

Figure 11: Solutions when $\Omega = -0.1$ and $\eta = 0.024$; Hopf bifurcation occured.

Now we will examine the value of $\Omega = -0.17$. First we will use injection strength of $\eta = 0.03$.

The roots of the cubic equation for N_s are (1.12)

$$\begin{aligned} &0.99990261662197 \\ &-0.03264361600329 + 0.00337968870960\mathtt{i} \\ &-0.03264361600329 - 0.00337968870960\mathtt{i}. \end{aligned}$$

Again, we can check on Figure 3 that we are still below the saddle-node bifurcation curve, so we only have one real root for the cubic and one equilibrium position of the original differential equation system. The eigenvalues of the Jacobian (1.15) at the only real root are

$$\begin{aligned} &0.99990252231967 + 5.16951308368940\mathtt{i} \\ &0.99990252231967 - 5.16951308368940\mathtt{i} \\ &-0.00099987632187. \end{aligned}$$

This shows that this equilibrium solution is unstable, as the real part of the complex conjugate pair is positive. One solution starting close to this equilibrium is shown as a function of time and as a phase-space curve in the E-ψ-N-space on the next Figure.

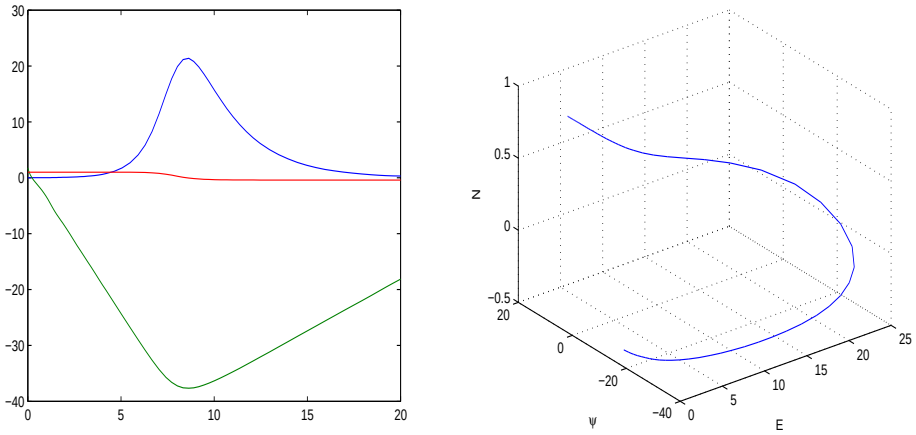

Figure 12: Solution when $\Omega = -0.17$ and $\eta = 0.03$.

Let us raise the injection level above the saddle-node curve now at this detuning value. We choose $\eta = 0.04$. We obtain that the roots of the cubic (1.12) are

$$\begin{aligned} &0.99982685733485 \\ &-0.03620465456931 \\ &-0.02900681815015. \end{aligned}$$

Again we see three real roots for N_s, which translates to three equilibrium solutions. One of the equilibria obtained from the saddle-node bifurcation is stable, the other unstable: the eigenvalues of the Jacobian (1.15) at the first steady state of the new pair are

$$\begin{aligned} &-0.00564245921773 + 0.05459638587469\mathtt{i} \\ &-0.00564245921773 - 0.05459638587469\mathtt{i} \\ &-0.06435857581256, \end{aligned}$$

and at the second steady state of the new pair are

$$\begin{aligned} &-0.04556131894487 + 0.06601823484648\mathtt{i} \\ &-0.04556131894487 - 0.06601823484648\mathtt{i} \\ &\ \ 0.02992424211137, \end{aligned}$$

which shows the validity of our claim about their stability properties. We also show time integration results at these equilibria.

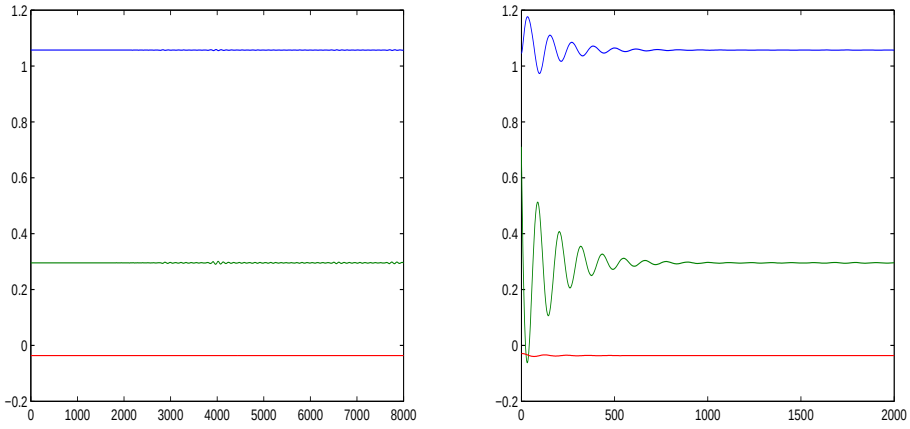

Figure 13: Solutions when $\Omega = -0.17$ and $\eta = 0.04$; saddle-node bifurcation equilibria.

The phase-space picture also shows that one of these new equilibria is unstable, the other stable: a solution starting close to the unstable is attracted to the stable one.

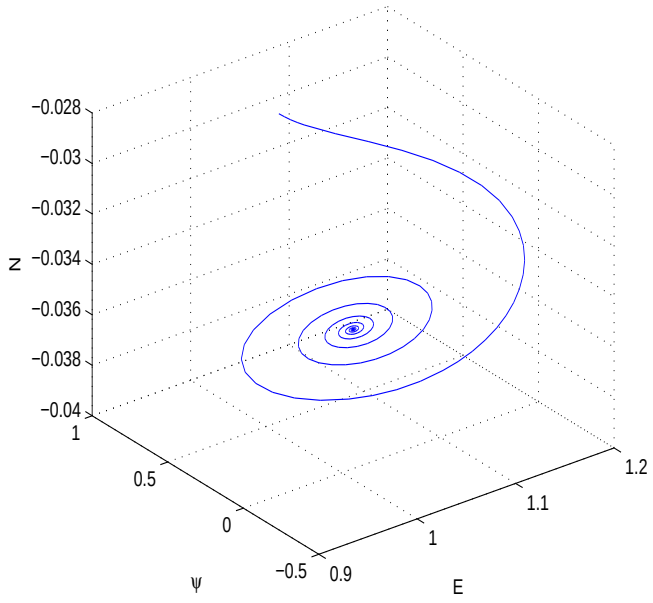

Figure 14: Phase-space plot when $\Omega = -0.17$ and $\eta = 0.04$; the solution leaves the unstable equilibrium and is attracted to the stable one.

If we raise the level of the injection above the Hopf bifurcation curve on Figure 6, we expect that the (up to this point) stable equilibrium obtained from the saddle-node bifurcation will lose its stability and become unstable as the complex pair of eigenvalues corresponding to this steady state will cross over to the positive real part half of the complex plane. We choose $\eta = 0.056$. We obtain that the roots of the cubic (1.12) are

$$\begin{aligned} &0.99966056868317 \\ -&0.04067485866032 \\ -&0.02437032540746. \end{aligned}$$

The eigenvalues at the second of these equilibria are now

$$\begin{aligned} &0.00033033469257 + 0.071913336683102\mathtt{i} \\ &0.00033033469257 - 0.071913336683102\mathtt{i} \\ -&0.08527604726951. \end{aligned}$$

By examining the eigenvalues we can observe that the equilibrium solution loses its stability. Time integration and phase-space plot at this equilibrium changes to the following:

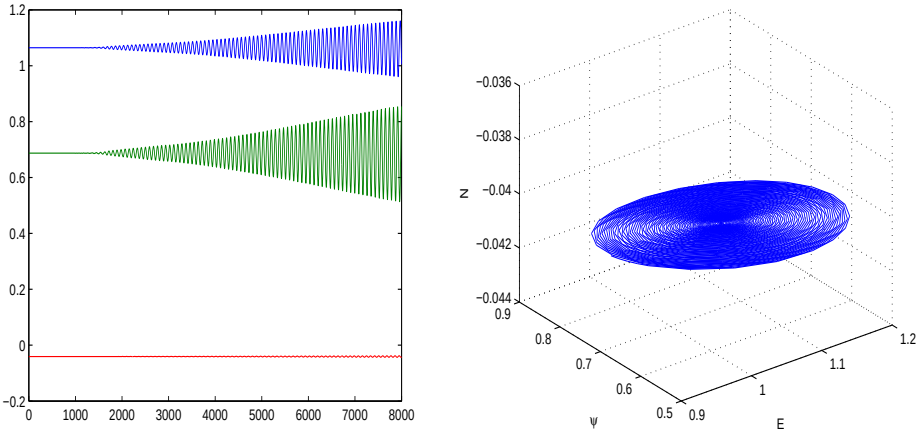

Figure 15: Solutions when $\Omega = -0.17$ and $\eta = 0.056$; Hopf bifurcation occured.

Let us raise now the injection strength to $\eta = 0.08$. According to Figure 6, at this level we cross back with the complex pair of eigenvalues and the equilibrium becomes stable again!

We obtain that the roots of the cubic (1.12) are

$$\begin{aligned} &0.99930697171325 \\ -&0.04577209583162 \\ -&0.01891949126625. \end{aligned}$$

The eigenvalues at the second of these equilibria are now

$$\begin{aligned} -&0.00074145242450 + 0.08839962050216\mathtt{i} \\ -&0.00074145242450 - 0.08839962050216\mathtt{i} \\ -&0.09336359384167. \end{aligned}$$

By examining the eigenvalues we can observe that the equilibrium solution regains its stability. Time integration and phase-space plot at this equilibrium changes to the following:

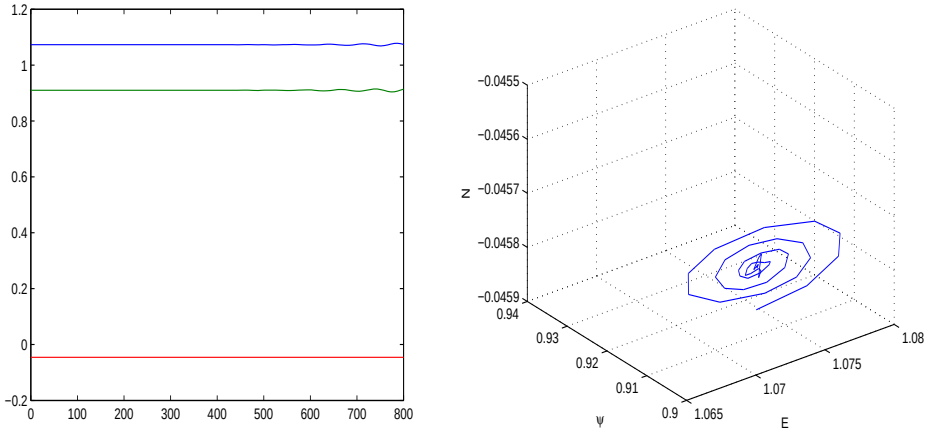

Figure 16: Solutions when $\Omega = -0.17$ and $\eta = 0.08$.

We will now examine some other detuning values, Ω and change the bifurcation parameter, η to show that the results are consistent again with the above analysis.

Let us examine a positive detuning value next; the stability curves we obtained are not symmetric in Ω.

Consider the value of the detuning $\Omega = 0.15$. Our bifurcation parameter is again the injection strength η. We start with $\eta = 0.025$.

The roots of the cubic equation for N_s are (1.12)

$$0.99992353146301$$
$$0.02888438811465 + 0.00266507382977\mathtt{i}$$
$$0.02888438811465 - 0.00266507382977\mathtt{i}.$$

We can check on Figure 3 that we are still below the the saddle-node bifurcation curve, so we only have on real root for the cubic and one equilibrium position of the original differential equation system. The eigenvalues of the Jacobian (1.15) at the only real root are

$$0.99992345272302 + 4.84961765683169\mathtt{i}$$
$$0.99992345272302 - 4.84961765683169\mathtt{i}$$
$$-0.00099989350163.$$

This shows that this equilibrium solution is unstable, as the real part of the complex conjugate pair is positive. One solution starting close to this equilibrium is shown as a function of time and as a phase-space curve in the E-ψ-N-space on the next Figure.

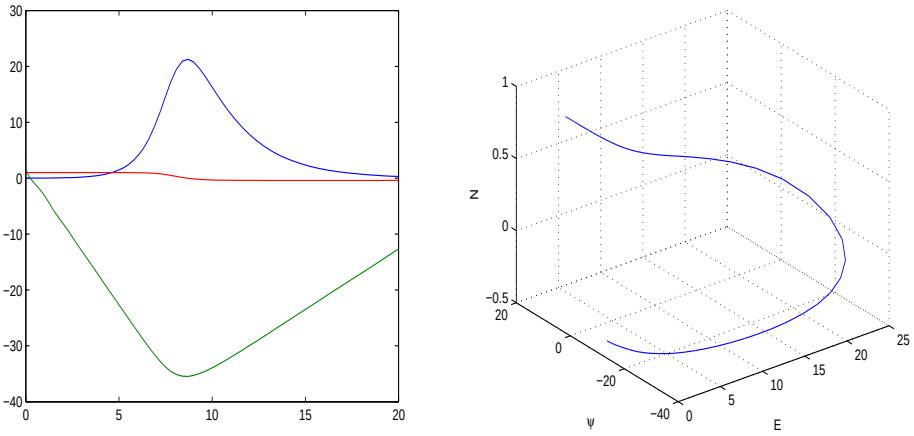

Figure 17: Solution when $\Omega = 0.15$ and $\eta = 0.025$.

Let us raise the injection level above the saddle-node curve now at this detuning value. We choose $\eta = 0.03$. We obtain that the roots of the cubic (1.12) are

$$0.99988988014550$$
$$0.03100345841770$$
$$0.02679896912911.$$

We can see that now we have three real roots for N_s, which translates to three equilibrium solutions. In this case, though, we have a different kind of behavior; here the eigenvalues for the two new equilibria are the following: at the first steady state of the new pair are

$$\begin{aligned} &0.00562672560277 + 0.04667117535350\mathtt{i} \\ &0.00562672560277 - 0.04667117535350\mathtt{i} \\ &0.04792862527105, \end{aligned}$$

and at the second steady state of the new pair are

$$\begin{aligned} &0.03714867775250 + 0.05601409383101\mathtt{i} \\ &0.03714867775250 - 0.05601409383101\mathtt{i} \\ -&0.02354680322873, \end{aligned}$$

which shows that in this case both new equilibria are unstable. The sign change happens only in a one dimensional sense, so the saddle-node bifurcation scenario is different here. (The classical saddle-node bifurcation is a one dimensional concept.) So the behavior described on Figure 7 will not happen for positive detuning. We show the solutions as well on the next figure.

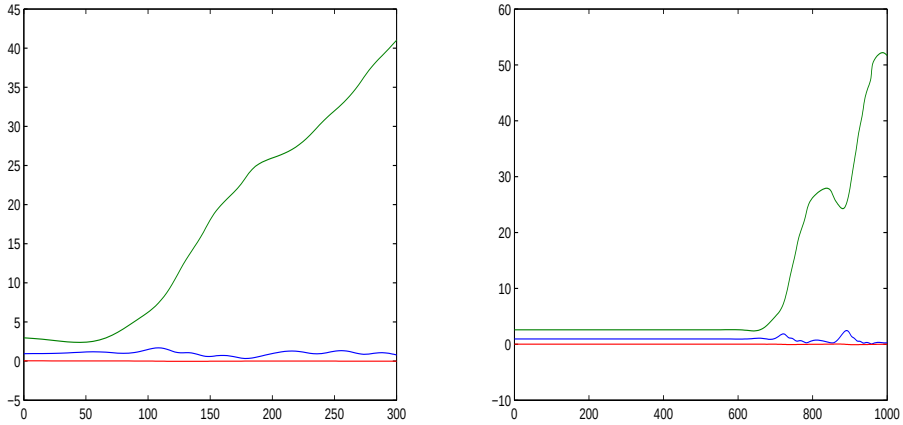

Figure 18: Solutions when $\Omega = 0.15$ and $\eta = 0.03$; saddle-node bifurcation equilibria.

So our numerical results also show that some of the analytical stability conclusions hold for negative detuning only; for the corresponding positive values of Ω the stability analysis will not be valid because in this case in the Routh-Hurwitz criterion $A_1 < 0$ for both new equilibria, as we mentioned earlier.

Chapter 3

Appendix

3.1 Codes in Maple

We used Maple to create the implicit plot describing the saddle-node bifurcation and the parametric plots describing the real root crossing and the Hopf bifurcation on the Ω-η plane. The codes are easy to modify for different parameter values.

The code for the saddle-node picture:

```
>alpha:=5;
>P:=1;
>a:=1+alpha^2;
>b:=-P-P*alpha^2-2*alpha*Omega;
>c:=2*eta^2+2*alpha*Omega*P+Omega^2;
>d:=eta^2-P*Omega^2;
>g:=(-b-sqrt(b^2-3*a*c))/(3*a);
>with(plots):implicitplot(a*g^3+b*g^2+c*g+d=0,Omega=-0.4..0.4,eta=0..0.1);
```

The code for the Hopf bifurcation picture:

```
>alpha:=5;
>P:=1;
```

```
>epsilon:=0.001;
>f1:=(2*alpha*s*(1+s)-alpha*P)/(1+2*P)+sqrt(alpha^2*(P-s)^2*
   (1+2*s)^2-(1+2*P)*((1+2*P)*s^2-2*s*(P-s)*(1+2*s)))
   /(1+2*P);
>f2:=sqrt((P-s)/(1+2*s))*sqrt(s^2+(f1-alpha*s)^2);
>f3:=alpha*t-2*epsilon*alpha*(P-t)/(4*t)+sqrt(4*epsilon^2*
   alpha^2*(P-t)^2-
   8*t*(2*t*epsilon*(P-t)+2*t^3+(1+2*P)/(1+2*t)*
   (2*t*epsilon^2*(1+2*P)/(1+2*t)-4*t^2*epsilon-2*epsilon^2*
   (P-t))))/(4*t);
>f4:=sqrt((P-t)/(1+2*t))*sqrt(t^2+(f3-alpha*t)^2);
>plot([[f1(s),f2(s),s=-0.1..0.1],[f3(t),f4(t),t=-0.1..0.1]],
   color=[blue,red],view=[-0.2..0.2,0..0.1]);
```

3.2 Codes in MATLAB

We used MATLAB to numerically investigate the cubic polynomial for N_s, to find the eigenvalues for the Jacobian at the equilibrium positions and to numerically time integrate our differential equation system. For the time integration we used the MATLAB routine `ode45`, which utilizes a Dormand-Price method and is a medium order method to solve non-stiff differential equations.

The MATLAB `.m` file for obtaining the roots of the cubic (1.12):

```
format long;
alpha=5;
P=1;
Omega=-0.1;
eta=0.02;
T=1000;
f=[(1+alpha^2) (-P-(alpha^2)*P-2*alpha*Omega)
   ((2*eta^2)+2*alpha*Omega*P+Omega^2) (eta^2-P*Omega^2)];
a=roots(f)
```

The MATLAB `.m` file for obtaining the eigenvalues at a given root of (1.12):

```
format long;
N=a(2);
E=sqrt((P-N)/(1+2*N));
A=[N E*(alpha*N-Omega) E;(Omega-alpha*N)/E N -alpha;-2*(1+2*N)*E/T
0 -(1+2*E^2)/T];
eig(A)
```

The MATLAB `.m` file for time integration of our system:

```
format long;
N=a(2);
E=sqrt((P-N)/(1+2*N));
psi=acos(-N*E/eta);
[t,x]=ode45(@injection,[0,8000],[E;psi;N],[],alpha,P,Omega,eta,T);
plot(t,x);
```

This file uses the function `.m` file `injection.m`, which contains the differential equation system (1.3-1.4-1.5):

```
function xprime=injection(t,x,alpha,P,Omega,eta,T)
xprime=zeros(3,1);
xprime(1)=x(1)*x(3)+eta*cos(x(2));
xprime(2)=Omega-alpha*x(3)-eta*sin(x(2))/x(1);
xprime(3)=(P-x(3)-(1+2*x(3))*x(1)^2)/T;
```

Bibliography

[1] Lang and Kobayashi Phase Equation, P.M. Alsing, V. Kovanis, A. Gavrielides, and T. Erneux, *Physical Review A*, **53** 4429-4434 (1996).

[2] Mechanism for period-doubling bifurcation in a semiconductor laser subject to optical injection, T. Erneux, V. Kovanis, A. Gavrielides and P. Alsing, *Physical Review A*, **53** 4372-4380 (1996).

[3] *Dynamical Diversity: Optical Feedback Effects on Semiconductor Lasers*, D. Kane and A. Shore [Eds], John Wiley & Sons (2005).

[4] *Perturbation Methods in Applied Mathematics*, J. Kevorkian, J.D. Cole, Springer-Verlag **AMS 34** (1981).

[5] External optical feedback effects on semiconductor injection laser properties, R. Lang and K. Kobayashi, *IEEE J. Quantum Electron.* **16**(3), 347-355 (1980).

[6] *A First Course in the Qualitative Theory of Differential Equations*, J.H. Liu, Prentice Hall (2003).

[7] Hopf bifurcation subject to a large delay in a laser system, D. Pieroux, T. Erneux, A. Gavrielides and V. Kovanis, *SIAM Review* **45** 523-540 (2003).

[8] Semiconductor lasers with optical injection and feedback, G.H.M Van Tartwijk and D. Lenstra *Quantum Semiclass. Opt.* **7**, 87-143 (1995).

[9] *Intorduction to Applied Nonlinear Dynamical Systems and Chaos*, S. Wiggins, Springer-Verlag **TAM 2** (1990).